Calcium-carboxyl intra-bridging during interfacial polymerization: A novel strategy to improve antifouling performance of thin film composite membranes

Xiujuan Hao[†,1], Shanshan Gao[‡,1], Jiayu Tian[†,‡,*], Yan Sun[†], Fuyi Cui[§], Chuyang Y. Tang [,⊥,#,*]

[†]State Key Laboratory of Urban Water Resource and Environment, Harbin Institute of Technology, Harbin 150090, China

[‡]School of Civil Engineering and Transportation, Hebei University of Technology, Tianjin 300401, China

[§]College of Urban Construction and Environmental Engineering, Chongqing University, Chongqing 400044, China

UNESCO Centre for Membrane Science and Technology, School of Chemical Engineering, University of New South Wales, Sydney, New South Wales 2052, Australia

[⊥] UNSW Water Research Centre, School of Civil and Environmental Engineering, University of New South Wales, Sydney, New South Wales 2052, Australia

[#]Department of Civil Engineering, the University of Hong Kong, Pokfulam Road, Hong Kong S.A.R., China

[*] Corresponding authors. E-mail address: tjy800112@163.com; tangc@hku.hk.

[1] These authors contributed equally to this work.

24 **TABLE OF CONTENTS**

25

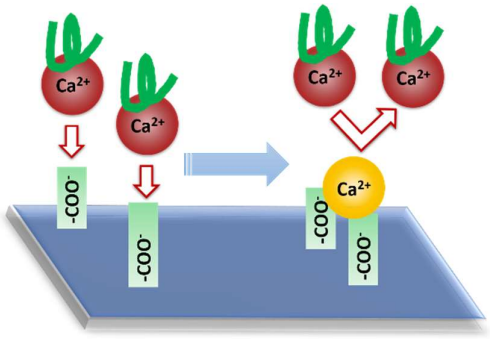

26

ABSTRACT

This study reports a novel intra-bridging strategy to improve the antifouling performance of a thin-film composite (TFC) membrane. We demonstrate that the addition of Ca^{2+} during the interfacial polymerization reaction led to the formation of stable Ca^{2+}-carboxyl complexes within the polyamide rejection layer. This intra-bridging of carboxyl groups by Ca^{2+} effectively sequestrated them, reducing their availability for binding divalent metal ions in the aqueous solution and for forming foulant-metal-membrane inter-bridges. Membrane fouling and cleaning experiments confirmed improved flux stability and fouling reversibility for the Ca^{2+} modified membranes. The greatly enhanced antifouling performance of these membranes, together with their better surface hydrophilicity and greater water permeability, makes the intra-bridging approach highly attractive in overcoming the classical permeability-selectivity-antifouling tradeoff. Our findings pave a new direction for synthesizing high-performance TFC membranes.

INTRODUCTION

Reverse osmosis membranes applied for desalination and water reuse are dominated by thin film composite (TFC) polyamide chemistry.[1-3] These membranes comprise a thin polyamide rejection layer on a porous support layer, in which the polyamide rejection layer determines not only the membrane separation properties but also their fouling propensity.[2, 4] Although the state-of-the-art TFC membranes possess desirable combinations of salt rejection and water permeability, their polyamide chemistry is often prone to membrane fouling.[1-6]

One of the key factors contributing to TFC membranes' vulnerability to fouling is the extensive presence of carboxyl groups on their surface.[4, 7-14] During the interfacial polymerization (IP) reaction of amine and acyl chloride monomers for the fabrication of TFC membrane (e.g., 1,3-phenylenediamine (MPD) and 1,3,5-benzenetricarbonyl trichloride (TMC), respectively), the unreacted acyl chlorides in the polyamide matrix rapidly hydrolyze into carboxyl groups.[7, 8, 14-16] These carboxyl groups are susceptible to organic fouling in the presence of divalent ions such as Ca^{2+} (Figure 1a).[17-24] Ca^{2+} ions bind to the carboxyl groups on the membrane surface and those of the organic foulants to form membrane-Ca^{2+}-organic bridges (referred as the inter-bridges in the current study), which often initiates severe foulant accumulation on the membrane surface.[17, 25] The presence of carboxyl groups also promotes biofouling[26, 27] and scaling[28, 29]. Although surface modifications methods such as coating or grafting an antifouling surface layer[30-32] can address this issue, it is often at the expense of reduced membrane permeability, higher cost and/or complex procedures.

For the first time, we propose a novel strategy to address the poor fouling performance of TFC membranes by sequestrating their carboxyl groups (Figure 1b). We hypothesize that the ability of carboxyl groups for promoting membrane-Ca^{2+}-organic inter-bridges

can be significantly weakened by "pre-occupancy" of these vulnerable sites during the membrane formation stage. Specifically, we demonstrate this idea with the simple addition of Ca^{2+} into the MPD monomer solution before performing the IP reaction. The presence of Ca^{2+} during the IP reaction promotes the formation of carboxyl-Ca^{2+}-carboxyl bridges within the polyamide layer. This intra-bridging by Ca^{2+} pre-occupies the carboxyl groups in the polyamide layer, making them unavailable to the formation of inter-bridges with foulants and thus minimizing membrane fouling propensity.

In the current study, we prepared a Ca^{2+}-intra-bridged TFC membrane and systematically characterized its surface composition, separation properties, and antifouling performance. We demonstrate superior antifouling performance of this novel membrane under reverse osmosis conditions. The novel intra-bridging strategy reported in this work provides an easy and efficient pathway for enhancing antifouling performance of TFC membranes.

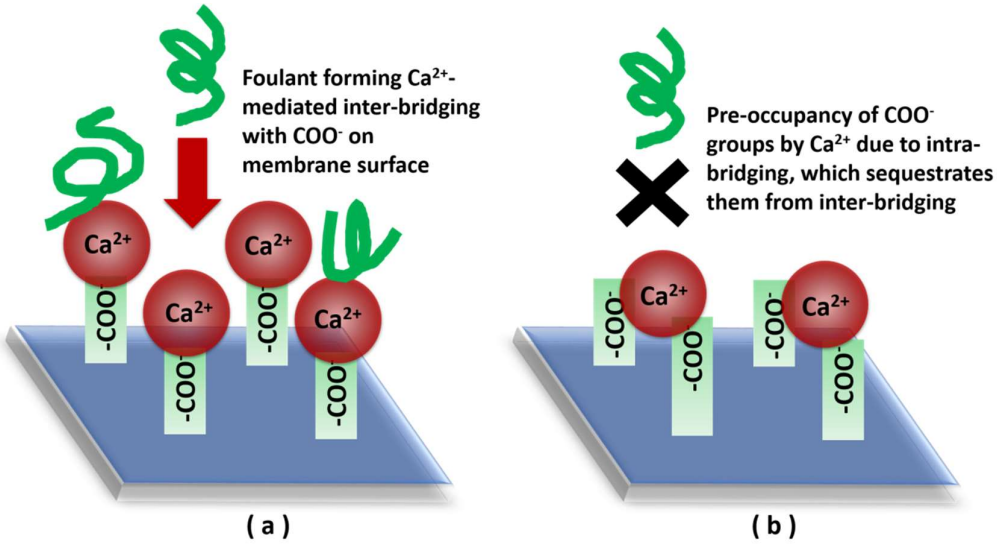

Figure 1. Illustration of anti-fouling mechanism of modified TFC membrane by Ca^{2+} addition during IP process. (a) TFC-control membrane. (b) Ca^{2+}-modified TFC membrane.

MATERIALS AND METHODS

Materials and Chemicals. Unless otherwise specified, all chemicals and reagents used in this study were of analytical grade. Udel® polysulfone (PSf, Mn=143 kDa, η=1.01 dL g^{-1}) was obtained from Solvay as the polymer material. Solvent N-methyl-2-pyrrolidone (NMP, Sigma-Aldrich, >99.5%) and pore former diethylene glycol (DEG, Sigma-Aldrich, >99.0%) were used to fabricate the PSf substrate. MPD (Sigma-Aldrich, >99%) and TMC (Sigma-Aldrich, >98%) were employed to synthesize the polyamide active layer via interfacial polymerization. Sodium chloride (NaCl), calcium chlorides ($CaCl_2$), magnesium chloride ($MgCl_2$) and barium chloride ($BaCl_2$) were obtained from Tianjin Kemiou Chemical Reagent Co., Ltd., China. Ethylene glycol, diethylene glycol, and glucose were obtained from Tianjin Kemiou Chemical Reagent Co., Ltd., China. Milli-Q water with a resistivity of 18.2 MΩ cm was used to prepare all working solutions. For membrane fouling evaluation, sodium alginate (SA, Sigma-Aldrich) and tannic acid (TA, Sigma-Aldrich) were selected as the model organic foulants to represent polysaccharides and humic substances, respectively. The stock solutions for the foulants were prepared by dissolving the foulants' power in Milli-Q water. All stock solutions were kept in the dark at 4 °C and used within one month after their preparation.

Preparation of Ca^{2+}-inter-bridged TFC Membrane. To prepare the PSf substrate, the polymer (PSf, 15 wt.%), pore former (DEG, 17 wt.%) and solvent (NMP, 68 wt.%) were stirred for 12 h for complete dissolution. The polymer solution was then degassed for more than 24 h. The resultant homogeneous solution was spread on a glass plate with a casting knife of 100 μm in height. The nascent film was immediately immersed into a water bath at room temperature (23 °C) for 10 min. The resultant PSf substrate was washed thoroughly and stored in DI water before use.

Interfacial polymerization was performed on the PSf substrate.[33] The PSf substrate was first immersed in 3.4 wt.% MPD aqueous solution for 120 s. To allow Ca^{2+}-intra-bridging, different amount of $CaCl_2$ (0, 0.2, 0.5, 1.0 and 2.0 wt.%) were dosed in the MPD solution. After the MPD soaking step, the excess MPD solution was removed using an air knife. A 0.15 wt.% TMC n-hexane solution was then brought into contact with the MPD saturated substrate for 60 s to form the polyamide layer. The nascent membrane was cured in DI water at 90 °C for 120 s, then rinsed with a 200 ppm NaClO aqueous solution for 120 s, followed by rinsing with a 1000 ppm $NaHSO_3$ aqueous solution for 30 s. Finally, the prepared Ca^{2+}-modified TFC membranes were cured at 90 °C for 120 s and stored in DI water at 4 °C before testing. The resulting membranes were denoted as TFC-Ca^{2+} (W), where W is the concentration of $CaCl_2$ (in wt.%) dosed in the MPD solution (Table S1, Supporting Information S1).

Characterization of the Ca^{2+}-modified Membranes. The surface functional groups of the Ca^{2+}-modified membranes were characterized through Attenuated Total Internal Reflectance Fourier Transform Infrared Spectrometer (ATR-FTIR, Thermo ESCALAB250, USA). The chemical element composition of the Ca^{2+}-modified polyamide layer was analyzed using X-ray photoelectron spectroscopy (XPS, Axis Ultra DLD, Kratos X-ray Photoelectron Spectrometer). The surface hydrophilicity of the fabricated membrane was evaluated by a contact angle meter (SL200B, Solon Tech Co., Ltd., China). The zeta potential of the TFC membranes was measured by an electro kinetic analyzer (Anton Paar GmbH, Austria) with the streaming potential measurements. An atomic force microscope (AFM, BioScope, Veeco Inc.) was used to characterize the membrane surface morphology.

The carboxyl group density was measured by the toluidine blue (TBO) method

134 developed by Elimelech and co-workers.[7, 8] Briefly, membrane coupons of 2 cm^2 were
135 contacted with 2 mM TBO solution at pH 11 for 3 min. After rinsing with and
136 immersion in a dye-free NaOH solution (pH = 11) for more than 4 h, the membrane
137 coupons were placed into 10 mL of 0.2 M NaCl solutions at pH 2 for 30 min under
138 stirring to release the bound TBO into the solution. The resultant solutions were
139 analyzed by optical density at a 630 nm wavelength. Light absorption was converted to
140 TBO concentration to calculate the membrane surface carboxyl group density.[7, 8]
141
142 **Performance Evaluation of the Ca^{2+}-modified TFC Membranes.**
143 **Separation performance characterization**. The water permeability (A), salt
144 permeability (B), and salt rejection (R) of the TFC membranes were measured in a
145 crossflow reverse osmosis filtration setup at room temperature (23 ± 0.5 °C). Briefly, a
146 membrane (effective area of 15.89 cm^2) was first compacted with DI water at a cross
147 flow velocity of 8.5 cm/s ($Re \approx 174$) and an applied pressure of 20 bar until the permeate
148 flux became stable. The intrinsic water permeability coefficient, A, was then calculated
149 by dividing the measured water flux J_w by the applied pressure ΔP, i.e., $A = J_w/\Delta P$.
150 Subsequently, a 20 mM NaCl was introduced to the feed solution to determine the salt
151 rejection. The observed NaCl rejection, R, was calculated from $R = 1\text{-}C_P/C_f$, where the
152 permeate concentration C_P and the feed concentration C_f were both based on
153 conductivity measurements. Neutral hydrophilic molecules, including ethylene glycol,
154 diethylene glycol, and glucose (MW = 62.1, 106.1, and 180.2 Dalton, respectively),
155 were also used to evaluate the effect of membrane modification on the size exclusion
156 effect.[34-36] Rejection of each compound was determined using a feed concentration of
157 200 mg/L under a pressure of 20 bar, and both the feed and permeate concentration
158 were determined by total organic carbon tests.

Ca^{2+} adsorption tests. To verify the effect of intra-bridging on the sequestration of carboxyl groups, we performed Ca^{2+} adsorption tests for the TFC-control and TFC-Ca^{2+} (1.0) membranes. Membrane coupons with an area of 1.0×2.0 cm^2 were soaked in 15 mL 1 wt.% $CaCl_2$ solutions (pH adjusted to 3, 4, 5, and 7) at 4 °C. The water samples were collected at 1, 3, 5, and 7 days, and the amount of Ca^{2+} adsorbed on TFC-control and TFC-Ca^{2+} (1.0) membranes was quantified by an inductively coupled plasma optical emission spectrometer (ICP-OES, 5300DV, PerkinElmer). The average values from three membrane samples were reported.

Membrane fouling characterization.

Membrane fouling and cleaning were performed using sodium alginate (SA) and tannic acid (TA) as model organic foulants to represent polysaccharides and humic substances, respectively. Briefly, a new membrane was first equilibrated with the foulant-free background electrolyte (1 mM $CaCl_2$ + 47 mM NaCl) under pressure until a stable water flux achieved. To ensure that fouling behavior can be compared between different membranes, the applied pressure was adjusted to obtain an identical initial water flux of 22 LMH for all fouling experiments. To start membrane fouling, a foulant stock solution was added to the feed tank to reach a final feed foulant concentration of 200 mg/L of SA or TA. During the entire test, the following conditions were maintained: feed solution pH 7.2 ± 0.2, ionic strength of 50 mM (1 mM $CaCl_2$ + 47 mM NaCl), constant temperature of 23 ± 0.5 °C, and a cross flow velocity of 8.5 cm/s ($Re \approx 174$). Physical cleaning with DI water was also performed at the end of the fouling experiments to evaluate fouling reversibility.[37-39] Membrane cleaning involved DI water rinsing at the same cross-flow velocity of 8.5 cm/s for 60 min. After cleaning, pure water flux of the tested membrane was measured to calculate the flux recovery ratio. Each fouling and cleaning experiment was repeated at least twice using different

membrane coupons.

RESULTS AND DISCUSSION

Membrane Characterization. Figure 2 presents ATR-FTIR, XPS, contact angle and zeta potential results. The ATR-FTIR spectra (Figure 2a) of both the TFC-control and the Ca^{2+}-modified membranes show the characteristic peaks of fully aromatic polyamide: 1540 cm^{-1} (amide II peak, assigned to the bending vibration of −N−H), 1660 cm^{-1} (amide I peak, assigned to the stretching vibration of –C=O), and 1613 cm^{-1} (ascribed to the bending vibration of aromatic ring in the polyamide active layer).[16, 37] However, a new peak occurred at 1728 cm^{-1} (carbonyl group in stretching mode [40]) for the Ca^{2+}-modified membranes, which can be attributed to the complexation of Ca^{2+} with the carboxyl groups on the membrane surface. Consistent with the FTIR results, XPS results (Figure 2b and Table S2) confirmed increased presence of calcium (Ca2p peak at the binding energy of 348 eV) in the polyamide rejection layer in the order of TFC-control (0.0 %) < TFC-Ca^{2+} (0.2) (0.1 %) < TFC-Ca^{2+} (0.5) (0.3 %) < TFC-Ca^{2+} (1.0) (0.5 %). However, TFC-Ca^{2+} (2.0) had a lower Ca^{2+} content (0.3%) compared to TFC-Ca^{2+} (1.0), indicating that further increasing the $CaCl_2$ concentration was not effective for incorporating more Ca^{2+} in the polyamide layer.

Water contact angle (CA) measurements (Figure 2c) show improved surface hydrophilicity upon Ca^{2+} modification. The TFC-control membrane presents the most hydrophobic membrane surface with the water contact angle of 73.9°, which is in line with previously published data for a hand-cast polyamide membrane.[19] The water contact angle dropped sharply to 29.8° for TFC-Ca^{2+}(1.0), which is accompanied with a noticeably reduction in the surface roughness and a shift from leaf-like to nodular surface morphology (Figure 3). Although the underlining mechanism is not clearly

known, the dramatic changes in surface hydrophilicity and morphology may be ascribed to a significant change of the physiochemical environment within the Ca^{2+}-modified membranes (e.g., changed hydrogen bonding behavior and the ability of Ca^{2+} to accommodate hydration water molecules). In addition, our recent study revealed that the surface roughness of TFC polyamide membranes is controlled by the degassing of nanosized CO_2 gas bubbles from the aqueous amine solution.[41, 42] The formation of Ca^{2+}-carboxyl complexation in the current study may significantly change this degassing behavior and thus the surface morphology. Zeta potential (ζ) results show a less negative membrane surface with the increase of Ca^{2+} concentration in MPD aqueous solution up to 1 wt% (-19.4 ± 0. 9 mV for the TFC-Ca^{2+} (1.0) membrane vs. -28.6 ± 1.2 mV for the TFC-control membrane), which is attributed to the partial charge neutralization effect upon Ca^{2+}-carboxyl complexation.[43] To determine the density of the free carboxyl groups, the TBO method[7, 8] was used (Figure 2e). The TFC-Ca^{2+} (1.0) membrane had a carboxyl density of 16.9 ± 0.5 nm^{-2}, or approximately half of that of the TFC-control membrane. These results not only confirm the effectiveness on the sequestration of carboxyl groups by the Ca^{2+} intra-bridging strategy but also explain the reduced zeta potential for TFC-Ca^{2+} (1.0). Compared to TFC-Ca^{2+} (1.0), TFC-Ca^{2+} (2.0) had a rougher surface (Figure 3e,f), greater water contact angle (Figure 2c), and more negative surface charge (Figure 2d), which is consistent with its lower Ca^{2+} incorporation (Figure 2b and Table S2).

229

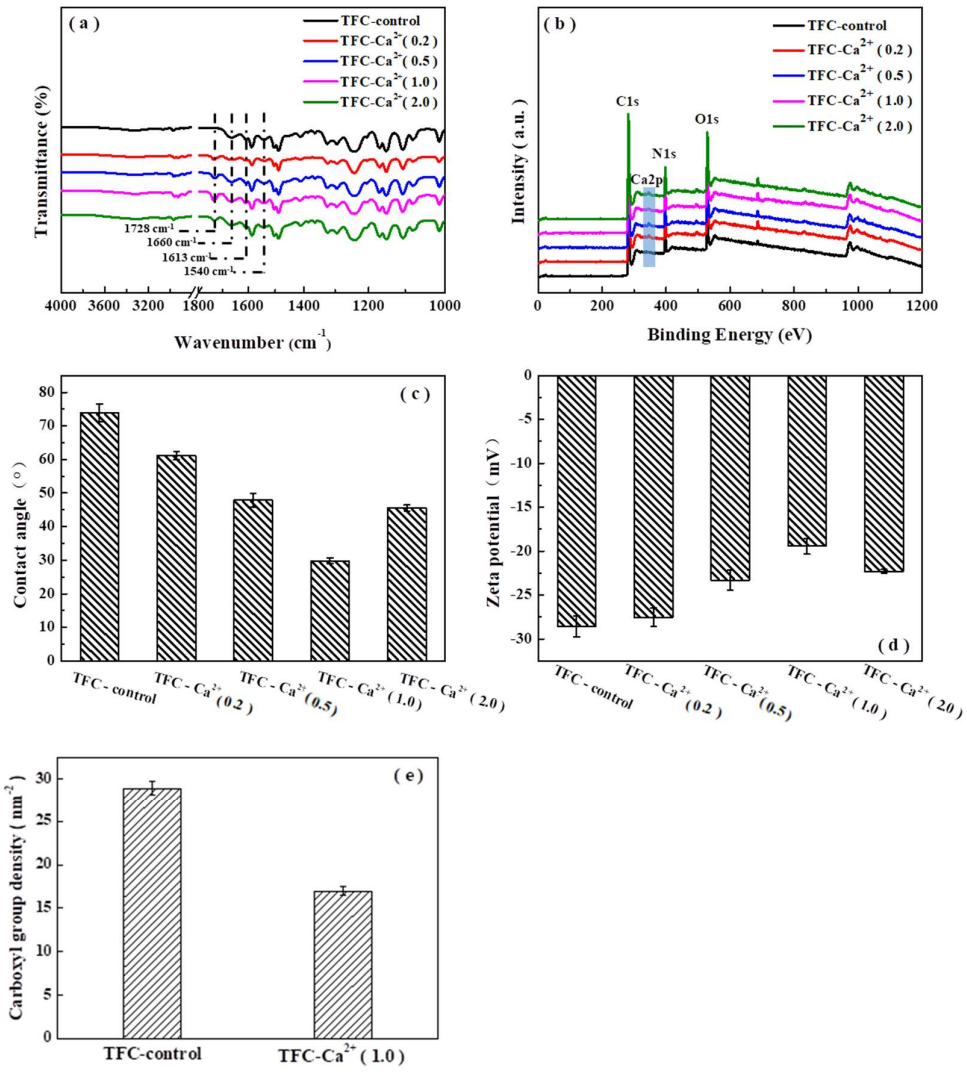

230

231 **Figure 2. Surface characterization of the TFC-control and Ca^{2+}-modified TFC membranes:**

232 **(a) ATR-FTIR spectra, (b) XPS spectra, (c) water contact angle results, (d) zeta potential**

233 **results (at pH 7.4), and (e) carboxyl group density.**

234

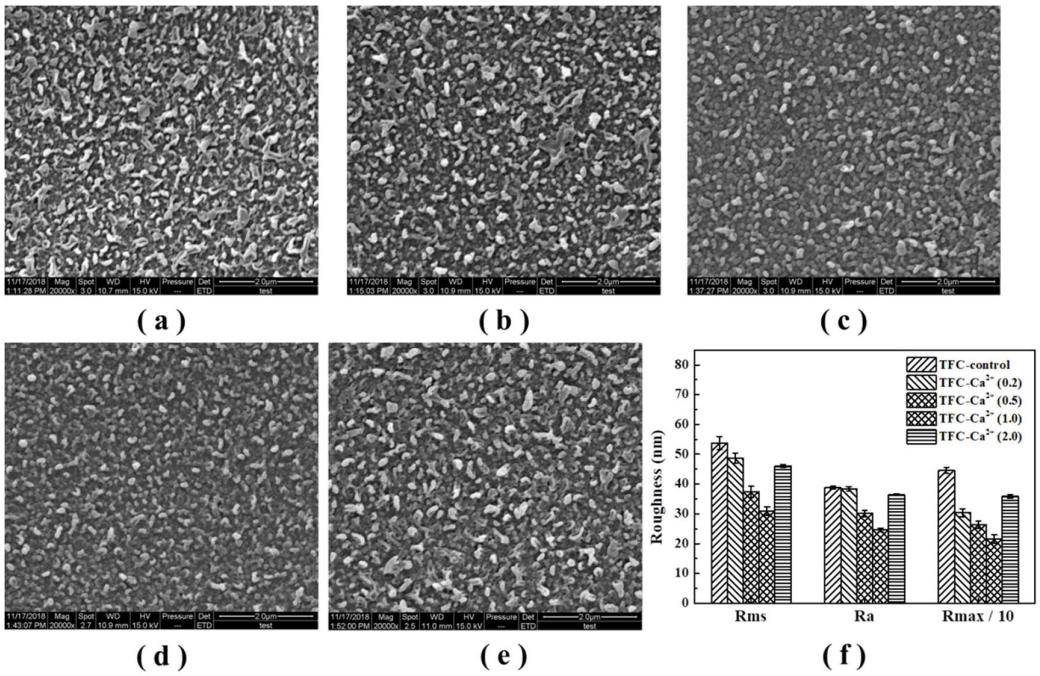

Figure 3. Microscopic characterization. SEM images of the polyamide active layer of (a) TFC-control, (b) TFC-Ca^{2+} (0.2), (c) TFC-Ca^{2+} (0.5), (d) TFC-Ca^{2+} (1.0), (e) TFC-Ca^{2+} (2.0), and (f) their AFM root mean square (Rms), average (Ra) and maximum (Rmax) surface roughness.

Performance of the Ca^{2+}-modified TFC Membranes. Table 1 presents the membrane separation properties (i.e., water permeability (A), salt permeability (B), and salt rejection (R)) obtained by reverse osmosis testing. The TFC-control membrane had the lowest A value of 1.70 ± 0.11 $L \cdot m^{-2} \cdot h^{-1} \cdot bar^{-1}$. In comparison, the TFC-Ca^{2+} (1.0) membrane show a higher water permeability of 2.44 ± 0.09 $L \cdot m^{-2} \cdot h^{-1} \cdot bar^{-1}$. The increase in water permeability is ascribed to the significantly improved hydrophilicity of the Ca^{2+}-modified polyamide layer (Figure 2c). Our results are consistent with the study by Wan et al.,[44] who performed interfacial polymerization on a calcium-chloride-dosed polyethersulfone substrate and found that the resulting polyamide became permeable.

The increase in water permeability was accompanied with an increase in salt

permeability (0.42 $Lm^{-2}h^{-1}$ for TFC-Ca^{2+} (1.0) vs. 0.37 $Lm^{-2}h^{-1}$ for TFC-control, Table 1). Nevertheless, all the membranes maintained comparable salt rejection (~98%). Salt rejection of TFC membranes are affected by the combined effects of size exclusion and charge repulsion. To assess the size exclusion effect, additional rejection tests were performed for TFC-control and TFC-Ca^{2+} (1.0) using three neutral hydrophilic molecules (ethylene glycol, diethylene glycol, and glucose, see Figure S1 in Supporting Information S2).[34-36] Since these molecular probes are neutral, their higher rejections by TFC-Ca^{2+} (1.0) suggest the formation of a tighter (i.e., more crosslinked) polyamide layer with enhanced size exclusion effect, which could be attributed to the formation of carboxyl-Ca^{2+}-carboxyl intra-bridging (i.e., metal-ligand complex) in addition to the covalent amide bonds. While the enhanced size exclusion effect had the tendency to increase salt rejection, the charge neutralization induced by the intra-bridging (Figure 2d) would reduce the charge repulsion effect with a negative impact on salt rejection. As a result of these competing effects, the overall NaCl rejection was not significantly affected. Figure 4 compares the separation performance of the Ca^{2+}-modified membranes with commercial reverse osmosis membranes. The separation performance of TFC-Ca^{2+} (1.0) was on par with commercial benchmarks.[45]

Table 1 Transport Properties of the TFC-control membrane and the Ca^{2+}-modified membranes.

Sample	Water permeability (A, $Lm^{-2}h^{-1}bar^{-1}$)	Salt permeability (B, $Lm^{-2}h^{-1}$)	Salt rejection (R, %)
TFC-control	1.70 ± 0.11	0.37 ± 0.06	98.1 ± 0.5
TFC-Ca^{2+} (0.2)	1.72 ± 0.10	0.39 ± 0.09	98.0 ± 0.3
TFC-Ca^{2+} (0.5)	1.93 ± 0.13	0.39 ± 0.10	97.7 ± 0.3
TFC-Ca^{2+} (1.0)	2.44 ± 0.09	0.42 ± 0.05	97.9 ± 0.3
TFC-Ca^{2+} (2.0)	1.97 ± 0.15	0.40 ± 0.07	98.0 ± 0.2

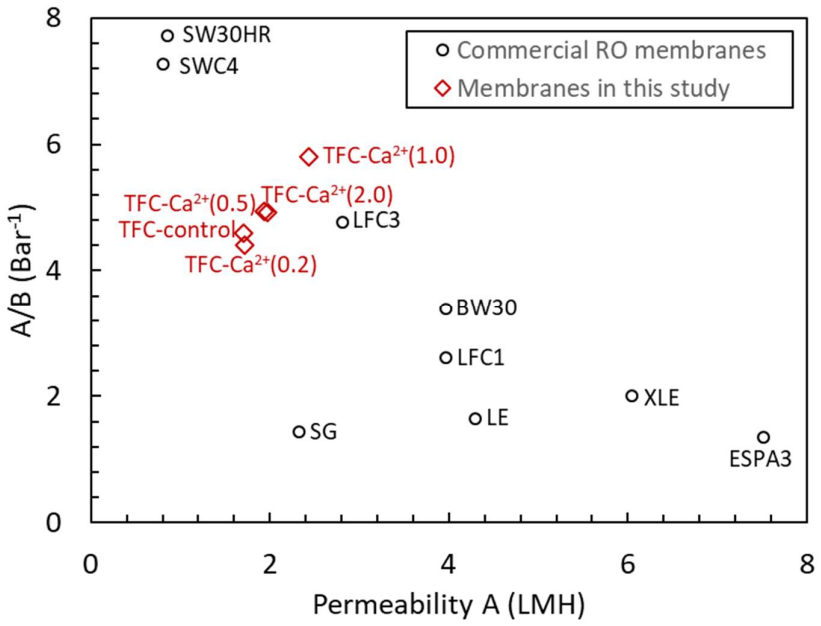

Figure 4. Benchmarking performance of the Ca^{2+}-modified membranes with commercial reverse osmosis membranes. The separation properties of commercial RO membranes were obtained from references [45, 46].

Antifouling Capability of the Ca^{2+}-modified Membranes. Figure 5 presents the fouling behavior of the TFC-control membrane and the TFC-Ca^{2+} (1.0) membrane

using a feed solution containing 200 mg/L sodium alginate (SA) or tannic acid (TA). The control membrane experienced significant flux decline (Figure 5a,b). In contrast, the Ca^{2+}-modified TFC membranes showed significantly improved flux stability. The TFC-Ca^{2+} (1.0) membrane exhibits only a mild flux decline of 13.2% for sodium alginate, compared to 24.8% for the TFC-control membrane (Figure 5a). A similar trend was observed when tannic acid was used as a model foulant (Figure 5b). The reduced fouling tendency of the Ca^{2+}-modified membranes can be attributed to the sequestration of the carboxyl groups due to their intra-bridging with Ca^{2+} (Figure 1), in addition to the more hydrophilic and smoother membrane surfaces.

Fouling reversibility was evaluated by cleaning the fouled membrane with DI water for 60 min. Compared to the control membrane, the TFC-Ca^{2+} (1.0) membrane had more reversible fouling, with 94.4% and 98.2% of the water flux recovered using sodium alginate and tannic acid as model foulants, respectively. Since TFC polyamide membrane is also the dominant membrane type used for osmotically-driven membrane process,[47-51] we further evaluated the antifouling performance of the calcium modified membranes under forward osmosis testing conditions.[13, 24, 52] Figure S3 and S4 (Supporting Information 3) clearly demonstrate improved flux stability for the TFC-Ca^{2+} (1.0) membrane even under forward osmosis fouling. Once again, this superior fouling reversibility can be explained by of the sequestration of the carboxylic groups for the Ca^{2+}-modified membranes, which weakens the binding between the polyamide layer and the foulants.

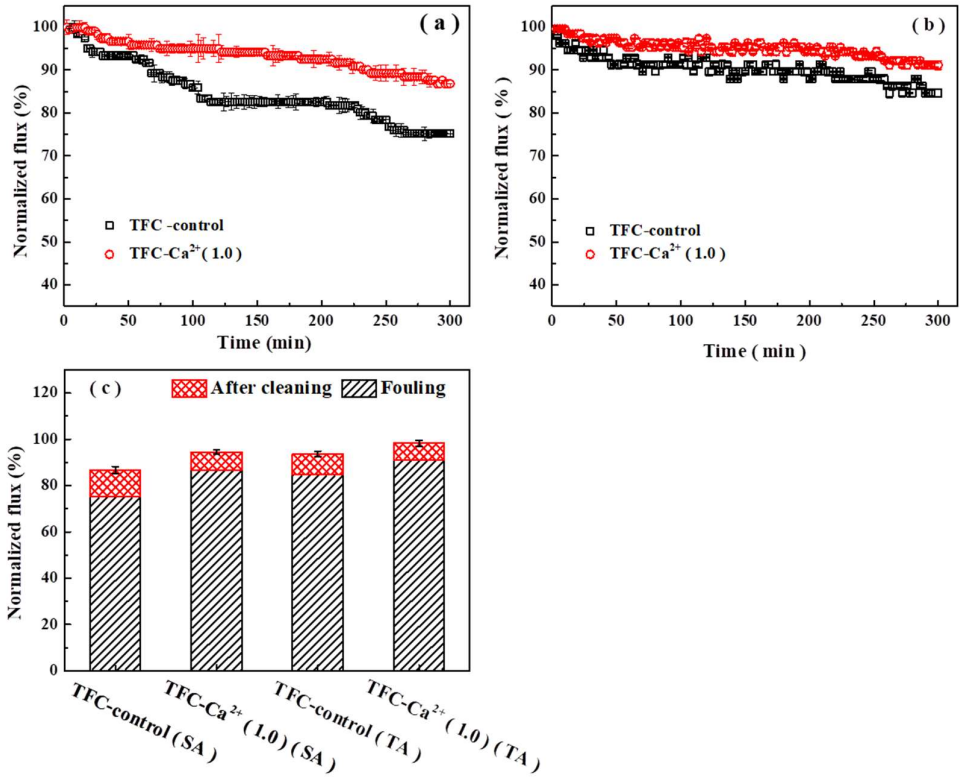

Figure 5. Reverse osmosis membrane fouling and fouling reversibility for the TFC-control and TFC-Ca^{2+} (1.0) membranes using sodium alginate (SA, 200 mg/L) and tannic acid (TA, 200 mg/L) as model foulants. (a) SA fouling tests; (b) TA fouling tests; and (c) fouling reversibility tests. An identical initial water flux of 22 LMH was used for all fouling experiments. Fouling reversibility was evaluated by cleaning the fouling membranes with DI water under crossflow conditions. Error bars are based on the range of the two repeated tests.

To further confirm the sequestration of carboxyl groups by the intra-bridging strategy, we investigated the ability of the TFC-control and TFC-Ca^{2+} (1.0) membranes to adsorb divalent ions (Ca^{2+}, Mg^{2+}, and Ba^{2+}) from the bulk solution. Ca^{2+} uptake (Figure 6) was measured under low to neutral pH (pH 3 - 7), since it is more easily leached (or less

tightly bound) under these conditions.[53, 54] The Ca^{2+} uptake by the TFC-control membrane was approximately 42.3 μg/cm^2, which is an order of magnitude greater than that by the TFC-Ca^{2+}(1.0) membrane (approximately 3.4 μg/cm^2). Similar trends were observed for the uptake of Mg^{2+} and Ba^{2+}, respectively (Supporting Information S4.1). In the presence of these divalent ions, the TFC-Ca^{2+}(1.0) membrane once again had better antifouling performance compared to the TFC-control membrane (Supporting Information S4.2). These results provide strong evidence that the intra-bridging approach was highly effective in reducing the availability of the carboxyl groups contained in the TFC-Ca^{2+}(1.0) membrane, which plays a critical role in enhancing its antifouling performance (Figure 5).

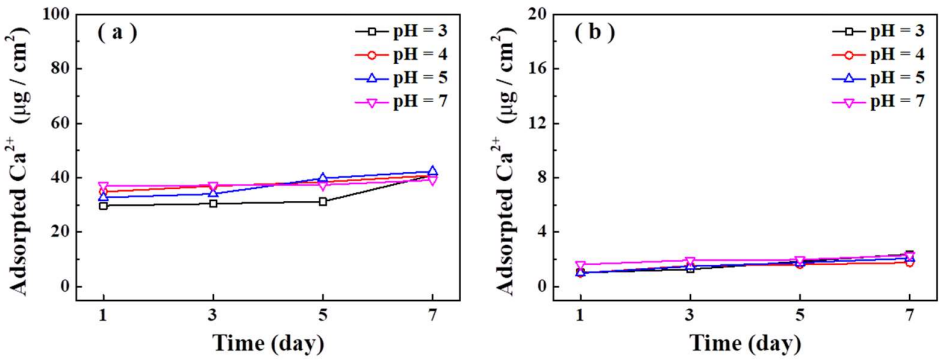

Figure 6. Uptake of Ca^{2+} by the TFC-control (a) and TFC-Ca^{2+} (1.0) membranes (b) by immersing them in a 1 wt.% $CaCl_2$ solution.

Membrane Stability. To evaluate the stability of the Ca^{2+}-modified membrane, we performed Ca^{2+} leaching tests for the TFC-Ca^{2+} (1.0) membrane in aqueous solutions at pH 3, 4, 5 and 7 over a 7-day period (Figure S7 in Supporting Information S5). Even at the lowest pH of 3, the released Ca^{2+} was significantly less than that of the total Ca^{2+} contained in the membrane. Additional leaching tests in the presence of high salinity

(0.1 or 1 M NaCl) or a strong chelating agent (1, 10, or 100 mM ethylenediaminetetraacetic acid (EDTA)) show the membrane was able to maintain its stability (Table S6 in Supporting Information S5). Our results imply the formation of highly stable Ca^{2+}-carboxyl complexes, which is likely caused by the binding of Ca^{2+} to multiple -COO^- sites within the membrane. According to Stumm and Morgen[55], metal binding to adjacent ligands can increase the stability constant by orders of magnitude.

IMPLICATIONS

We developed a simple and green modification method for preparation of antifouling TFC membranes. For the first time, we show compelling evidence of significantly improved antifouling performance by forming Ca^{2+}-carboxyl intra-bridging, which sequestrated these venerable groups to mitigate fouling. The Ca^{2+}-modified membrane also exhibits enhanced surface hydrophilicity and water permeability without scarifying its rejection. An added advantage of the intra-bridging is that the addition of $CaCl_2$ during interfacial polymerization can be easily realized within existing membrane production lines. Thus, the intra-bridging approach provides a simple and cost-effective way to overcome the longstanding permeability-rejection-antifouling tradeoff [45, 56, 57]

In the current study, the Ca^{2+}-modified membranes show high stability even in the presence of a strong chelating agent EDTA, which implies that Ca^{2+} is tightly bound in the polyamide matrix by forming complex with multiple carboxyl groups. This type of

carboxyl-Ca^{2+}-carboxyl bonding is critical to make both calcium and carboxyl groups unavailable to fouling. In contrast, pre-soaking a non-modified TFC membrane in $CaCl_2$ is not effective for fouling mitigation (Supporting Information 4.3). In the latter case, the absorbed Ca^{2+}, if not bound to multiple carboxyl groups in the polyamide, can still form membrane-Ca^{2+}-foulant inter-bridges. Future studies may explore alternative methods (such as the use of other divalent or multivalent metal ions) to further improve the carboxyl sequestration efficiency.

ASSOCIATED CONTENT

The Supporting Information is available free of charge on the ACS Publications website:

S1. The casting solution compositions of Ca^{2+}-modified membranes; S2. Characterization of the Ca^{2+}-modified membranes; S3. Forward osmosis (FO) results; S4. Additional evidences of the sequestration effect for the Ca2+-modified membranes; S5. Membrane stability.

AUTHOR INFORMATION

Corresponding Authors

*(C.Y.T.) Phone: +852 2859 1976; fax: +852 2559 5337; e-mail: tangc@hku.hk.

*(J.T.) Phone: +86 451 86282100; fax: +86 451 86282100; e-mail: tjy800112@163.com.

Notes

The authors declare no competing financial interest.

ACKNOWLEDGMENTS

This work was supported by the National Natural Science Foundation of China (No. 51678187) and the Postdoctoral Scientific Research Developmental Fund of Heilongjiang Province (No. LBHQ16109).

REFERENCES

1. Elimelech, M.; Phillip, W. A. The future of seawater desalination: Energy, technology, and the environment. *Science* **2011,** *333* (6043), 712-717.
2. Misdan, N.; Lau, W. J.; Ismail, A. F. Seawater Reverse Osmosis (SWRO) desalination by thin-film composite membrane-Current development, challenges and future prospects. *Desalination* **2012,** *287*, 228-237.
3. Tang, C. Y.; Yang, Z.; Guo, H.; Wen, J. J.; Nghiem, L. D.; Cornelissen, E. Potable Water Reuse through Advanced Membrane Technology. *Environ. Sci. Technol.* **2018,** *52* (18), 10215-10223.
4. Tang, C. Y.; Chong, T. H.; Fane, A. G. Colloidal interactions and fouling of NF and RO membranes: A review. *Adv. Colloid. Interfac.* **2011,** *164*, 126-143.
5. Guo, W.; Ngo, H. H.; Li, J. A mini-review on membrane fouling. *Bioresour. Technol.* **2012,** *122*, 27-34.
6. Li, X.; Cai, T.; Chung, T. S. Anti-Fouling behavior of hyperbranched polyglycerol-grafted poly(ether sulfone) hollow fiber membranes for osmotic power generation. *Environ. Sci. Technol.* **2014,** *48* (16), 9898-9907.
7. Mo, Y.; Tiraferri, A.; Yip, N. Y.; Adout, A.; Huang, X.; Elimelech, M. Improved antifouling properties of polyamide nanofiltration membranes by reducing the density of surface carboxyl groups. *Environ. Sci. Technol.* **2012,** *46* (24), 13253-13261.
8. Tiraferri, A.; Elimelech, M. Direct quantification of negatively charged functional groups on membrane surfaces. *J. Membr. Sci.* **2012,** *389*, 499-508.
9. She, Q.; Wang, R.; Fane, A. G.; Tang, C. Y. Membrane fouling in osmotically driven membrane processes: A review. *J. Membr. Sci.* **2016,** *499*, 201-233.
10. Zhang, R.; Liu, Y.; He, M.; Su, Y.; Zhao, X.; Elimelech, M.; Jiang, Z. Antifouling membranes for sustainable water purification: Strategies and mechanisms. *Chem. Soc. Rev.* **2016,** *45* (21), 5888-5924.
11. Liu, C.; Faria, A. F.; Ma, J.; Elimelech, M., Mitigation of Biofilm Development on Thin-Film Composite Membranes Functionalized with Zwitterionic Polymers and Silver Nanoparticles. *Environ. Sci. Technol.* **2017,** *51* (1), 182-191.
12. Qin, D.; Liu, Z.; Liu, Z.; Bai, H.; Sun, D. D. Superior Antifouling Capability of Hydrogel Forward Osmosis Membrane for Treating Wastewaters with High Concentration of Organic Foulants. *Environ. Sci. Technol.* **2018,** *52* (3), 1421-1428.
13. Mi, B.; Elimelech, M. Organic fouling of forward osmosis membranes: Fouling reversibility and cleaning without chemical reagents. *J. Membr. Sci.* **2010,** *348* (1-2), 337-345.
14. Tang, C. Y.; Kwon, Y.-N.; Leckie, J. O. Probing the nano- and micro-scales of reverse osmosis membranes—A comprehensive characterization of physiochemical properties of uncoated and coated membranes by XPS, TEM, ATR-FTIR, and streaming potential measurements. *J. Membr. Sci.* **2007,** *287* (1), 146-156.
15. Wang, Z.; Elimelech, M.; Lin, S. Environmental Applications of Interfacial Materials with Special Wettability. *Environ. Sci. Technol.* **2016,** *50* (5), 2132-2150.

16. Tang, C. Y.; Kwon, Y.-N.; Leckie, J. O. Effect of membrane chemistry and coating layer on physiochemical properties of thin film composite polyamide RO and NF membranes. I. FTIR and XPS characterization of polyamide and coating layer chemistry. *Desalination* **2009,** *242* (1-3), 149-167.
17. Li, Q.; Elimelech, M. Organic fouling and chemical cleaning of nanofiltration membranes: Measurements and mechanisms. *Environ. Sci. Technol.* **2004,** *38* (17), 4683-4693.
18. Xiang, Y.; Liu, Y.; Mi, B.; Leng, Y. Molecular dynamics simulations of polyamide membrane, calcium alginate gel, and their interactions in aqueous solution. *Langmuir* **2014,** *30* (30), 9098-9106.
19. Lu, X.; Romero-Vargas Castrillón, S.; Shaffer, D. L.; Ma, J.; Elimelech, M. In situ surface chemical modification of thin-film composite forward osmosis membranes for enhanced organic fouling resistance. *Environ. Sci. Technol.* **2013,** *47* (21), 12219-12228.
20. Tang, C. Y.; Kwon, Y.-N.; Leckie, J. O. Fouling of reverse osmosis and nanofiltration membranes by humic acid -- Effects of solution composition and hydrodynamic conditions. *J. Membr. Sci.* **2007,** *290* (1-2), 86-94.
21. Parida, V.; Ng, H. Y. Forward osmosis organic fouling: Effects of organic loading, calcium and membrane orientation. *Desalination* **2013,** *312*, 88-98.
22. Motsa, M. M.; Mamba, B. B.; D'Haese, A.; Hoek, E. M. V.; Verliefde, A. R. D. Organic fouling in forward osmosis membranes: The role of feed solution chemistry and membrane structural properties. *J. Membr. Sci.* **2014,** *460*, 99-109.
23. Lee, S.; Elimelech, M. Relating organic fouling of reverse osmosis membranes to intermolecular adhesion forces. *Environ. Sci. Technol.* **2006,** *40* (3), 980-987.
24. Mi, B.; Elimelech, M. Chemical and physical aspects of organic fouling of forward osmosis membranes. *J. Membr. Sci.* **2008,** *320* (1-2), 292-302.
25. Jin, X.; Huang, X.; Hoek, E. M. V. Role of specific ion interactions in seawater RO membrane fouling by alginic acid. *Environ. Sci. Technol.* **2009,** *43* (10), 3580-3587.
26. Zirehpour, A.; Rahimpour, A.; Arabi Shamsabadi, A.; Sharifian, M. G.; Soroush, M. Mitigation of Thin-Film Composite Membrane Biofouling via Immobilizing Nano-Sized Biocidal Reservoirs in the Membrane Active Layer. *Environ. Sci. Technol.* **2017,** *51* (10), 5511-5522.
27. Perreault, F.; Jaramillo, H.; Xie, M.; Ude, M.; Nghiem, L. D.; Elimelech, M. Biofouling Mitigation in Forward Osmosis Using Graphene Oxide Functionalized Thin-Film Composite Membranes. *Environ. Sci. Technol.* **2016,** *50* (11), 5840-5848.
28. Baoxia, M. I.; Elimelech, M. Gypsum scaling and cleaning in forward osmosis: Measurements and mechanisms. *Environ. Sci. Technol.* **2010,** *44* (6), 2022-2028.
29. Xie, M.; Gray, S. R. Gypsum scaling in forward osmosis: Role of membrane surface chemistry. *J. Membr. Sci.* **2016,** *513*, 250-259.
30. Liu, C.; Lee, J.; Ma, J.; Elimelech, M. Antifouling Thin-Film Composite Membranes by Controlled Architecture of Zwitterionic Polymer Brush Layer. *Environ. Sci. Technol.* **2017,** *51* (4), 2161-2169.

31. Zhang, X.; Tian, J.; Gao, S.; Zhang, Z.; Cui, F.; Tang, C. Y. In situ surface modification of thin film composite forward osmosis membranes with sulfonated poly(arylene ether sulfone) for anti-fouling in emulsified oil/water separation. *J. Membr. Sci.* **2017,** *527*, 26-34.
32. Xu, W.; Ge, Q. Novel functionalized forward osmosis (FO) membranes for FO desalination: Improved process performance and fouling resistance. *J. Membr. Sci.* **2018,** *555*, 507-516.
33. Zhang, X.; Tian, J.; Ren, Z.; Shi, W.; Zhang, Z.; Xu, Y.; Gao, S.; Cui, F. High performance thin-film composite (TFC) forward osmosis (FO) membrane fabricated on novel hydrophilic disulfonated poly(arylene ether sulfone) multiblock copolymer/polysulfone substrate. *J. Membr. Sci.* **2016,** *520*, 529-539.
34. Nghiem, L. D.; Schäfer, A. I.; Elimelech, M. Removal of Natural Hormones by Nanofiltration Membranes: Measurement, Modeling, and Mechanisms. *Environ. Sci. Technol.* **2004,** *38* (6), 1888-1896.
35. Yang, L.; She, Q.; Wan, M. P.; Wang, R.; Chang, V. W. C.; Tang, C. Y. Removal of haloacetic acids from swimming pool water by reverse osmosis and nanofiltration. *Water Res.* **2017,** *116*, 116-125.
36. Guo, H.; Deng, Y.; Yao, Z.; Yang, Z.; Wang, J.; Lin, C.; Zhang, T.; Zhu, B.; Tang, C. Y. A highly selective surface coating for enhanced membrane rejection of endocrine disrupting compounds: Mechanistic insights and implications. *Water Res.* **2017,** *121*, 197-203.
37. Zhao, H.; Qiu, S.; Wu, L.; Zhang, L.; Chen, H.; Gao, C. Improving the performance of polyamide reverse osmosis membrane by incorporation of modified multi-walled carbon nanotubes. *J. Membr. Sci.* **2014,** *450*, 249-256.
38. Valladares Linares, R.; Yangali-Quintanilla, V.; Li, Z.; Amy, G. NOM and TEP fouling of a forward osmosis (FO) membrane: Foulant identification and cleaning. *J. Membr. Sci.* **2012,** *421-422*, 217-224.
39. Liu, Y.; Mi, B. Combined fouling of forward osmosis membranes: Synergistic foulant interaction and direct observation of fouling layer formation. *J. Membr. Sci.* **2012,** *407-408*, 136-144.
40. Ye, G.; Lee, J.; Perreault, F.; Elimelech, M. Controlled Architecture of Dual-Functional Block Copolymer Brushes on Thin-Film Composite Membranes for Integrated "defending" and "attacking" Strategies against Biofouling. *ACS Appl. Mater. Inter.* **2015,** *7* (41), 23069-23079.
41. Ma, X.-H.; Yao, Z.-K.; Yang, Z.; Guo, H.; Xu, Z.-L.; Tang, C. Y.; Elimelech, M. Nanofoaming of polyamide desalination membranes to tune permeability and selectivity. *Environ. Sci. Technol. Lett.* **2018,** *5* (2), 123-130.
42. Ma, X.; Yang, Z.; Yao, Z.; Guo, H.; Xu, Z.; Tang, C. Y. Tuning roughness features of thin film composite polyamide membranes for simultaneously enhanced permeability, selectivity and anti-fouling performance. *J. Colloid. Interf. Sci.* **2019,** *540*, 382-388.

43. Tang, C. Y.; Kwon, Y. N.; Leckie, J. O. The role of foulant-foulant electrostatic interaction on limiting flux for RO and NF membranes during humic acid fouling-Theoretical basis, experimental evidence, and AFM interaction force measurement. *J. Membr. Sci.* **2009,** *326* (2), 526-532.
44. Wan, C. F.; Yang, T.; Gai, W.; Lee, Y. D.; Chung, T. S. Thin-film composite hollow fiber membrane with inorganic salt additives for high mechanical strength and high power density for pressure-retarded osmosis. *J. Membr. Sci.* **2018,** *555*, 388-397.
45. Tang, C. Y.; Kwon, Y.-N.; Leckie, J. O. Effect of membrane chemistry and coating layer on physiochemical properties of thin film composite polyamide RO and NF membranes II. Membrane physiochemical properties and their dependence on polyamide and coating layers. *Desalination* **2009,** *242* (1-3), 168-182.
46. Fane, A. G.; Tang, C. Y.; Wang, R. Membrane Technology for Water: Microfiltration, Ultrafiltration, Nanofiltration, and Reverse Osmosis. *Treatise on Water Science*, Wilderer, P., Ed. Academic Press: Oxford, **2011**; pp 301-335.
47. Wei, J.; Qiu, C.; Tang, C. Y.; Wang, R.; Fane, A. G. Synthesis and characterization of flat-sheet thin film composite forward osmosis membranes. *J. Membr. Sci.* **2011,** *372*, 292-302.
48. Yip, N. Y.; Tiraferri, A.; Phillip, W. A.; Schiffman, J. D.; Elimelech, M. High performance thin-film composite forward osmosis membrane. *Environ. Sci. Technol.* **2010,** *44* (10), 3812-3818.
49. Sukitpaneenit, P.; Chung, T. S. High performance thin-film composite forward osmosis hollow fiber membranes with macrovoid-free and highly porous structure for sustainable water production. *Environ. Sci. Technol.* **2012,** *46* (13), 7358-7365.
50. Liu, Q.; Qiu, G.; Zhou, Z.; Li, J.; Amy, G. L.; Xie, J.; Lee, J. Y. An Effective Design of Electrically Conducting Thin-Film Composite (TFC) Membranes for Bio and Organic Fouling Control in Forward Osmosis (FO). *Environ. Sci. Technol.* **2016,** *50* (19), 10596-10605.
51. Lu, X.; Arias Chavez, L. H.; Romero-Vargas Castrillón, S.; Ma, J.; Elimelech, M.Influence of active layer and support layer surface structures on organic fouling propensity of thin-film composite forward osmosis membranes. *Environ. Sci. Technol.* **2015,** *49* (3), 1436-1444.
52. Xie, M.; Bar-Zeev, E.; Hashmi, S. M.; Nghiem, L. D.; Elimelech, M. Role of Reverse Divalent Cation Diffusion in Forward Osmosis Biofouling. *Environ. Sci. Technol.* **2015,** *49* (22), 13222-13229.
53. Du, Y. J.; Wei, M. L.; Reddy, K. R.; Liu, Z. P.; Jin, F. Effect of acid rain pH on leaching behavior of cement stabilized lead-contaminated soil. *J. Hazard. Mater.* **2014,** *271*, 131-140.
54. Song, F.; Gu, L.; Zhu, N.; Yuan, H. Leaching behavior of heavy metals from sewage sludge solidified by cement-based binders. *Chemosphere* **2013,** *92* (4), 344-350.
55. Stumm, W.; Morgen, J. J. *Aquatic Chemistry, Chemical Equilibria and Rates in Natural Waters*. 3rd Edition ed.; John Wiley & Sons: New York, 1996.

547 56. Meng, J.; Cao, Z.; Ni, L.; Zhang, Y.; Wang, X.; Zhang, X.; Liu, E. A novel salt-
548 responsive TFC RO membrane having superior antifouling and easy-cleaning
549 properties. *J. Membr. Sci.* **2014,** *461*, 123-129.
550 57. Werber, J. R.; Deshmukh, A.; Elimelech, M. The Critical Need for Increased
551 Selectivity, Not Increased Water Permeability, for Desalination Membranes. *Environ.*
552 *Sci. Technol. Lett.* **2016,** *3* (4), 112-120.

553